Results in Engineering 17 (2023) 100800

Contents lists available at ScienceDirect

Results in Engineering

journal homepage: www.sciencedirect.com/journal/results-in-engineering

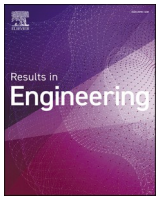

# Comparative study of electrodeposited copper nanoparticles on different substrates for their use in the reduction of nitrate ions

N. Zurita, S.G. García *

*Instituto de Ingeniería Electroquímica y Corrosión (INIEC), Departamento de Ingeniería Química, Universidad Nacional del Sur, Avda. Alem 1253, (8000) Bahía Blanca, Argentina*

ARTICLE INFO

*Keywords:*
Copper nanoparticles
Electrodeposition
Carbonaceous substrates
Nitrate

ABSTRACT

A comparative analysis of the electrodeposition of copper nanoparticles (CuNPs) was studied on highly oriented pyrolytic graphite (HOPG) and vitreous carbon (VC) substrates from solutions containing different supporting electrolytes ($Na_2SO_4$ and $H_2SO_4$).

Voltammetric results indicated the presence of a single cathodic process, corresponding to the reduction reaction of $Cu^{2+}$ ions to $Cu^{o}$, for the solutions studied, using the HOPG substrate. The solution containing $Na_2SO_4$ as supporting electrolyte was found to be more effective because the copper reduction process occurs at more positive potential values, reaching the highest current density. For the VC substrate, two cathodic processes were evidenced, with the formation of $Cu^{+}$ ions as intermediate species. As in the HOPG substrate, the use of the solution containing $Na_2SO_4$ showed the better behavior for copper electrodeposition, being the most favored process on VC. This behavior could be explained by considering the existence of structural defects in the VC, which would facilitate Cu nucleation.

The nucleation and growth kinetics of CuNPs on HOPG electrodes corresponded predominantly to a model including progressive nucleation on active sites, and diffusion controlled growth, presenting a good correlation with the scanning electron microscopy images. For VC substrates, the kinetics analysis did not yield conclusive results. Different morphological features of Cu deposits were observed on HOPG and VC, presenting the former a larger covered area.

The HOPG/CuNPs modified electrodes evidenced an enhancement in the catalytic activity towards the nitrate reduction reaction.

## 1. Introduction

In the last decades, the extensive use of nitrogenous fertilizers agricultural [1–4] areas has produced an increase in the level of nitrate in groundwater, reaching the water drinking resources. The risks associated with the consumption of water with higher concentrations of nitrate have been extensively studied [5–8]. The major is infant methaemoglobinaemia, which reduces the ability of red blood cells to release oxygen to tissues. The World Health Organization established that the limit value of nitrate concentration in drinking water for this affection is 50 mg/l from short-term exposure [9]. Furthermore, the intake of nitrate has been related to the increase in specific cancer [10, 11], even at nitrate levels in drinking water below the current drinking water standard [12]. Therefore it is evident the need to develop reliable techniques to detect and quantify the concentration of nitrate ions.

Actually, there is a wide variety of methods for nitrate detection and several reviews have been reported on the subject [13–15]. Among them, the chromatography is one of the conventional techniques with high sensitivity, detection range and detection limit. However, it is more expensive compared to other techniques, since it requires sample preparation and specialized equipment for accurate measurements [13]. Flow-injection analysis is a low cost and simple operation method used in laboratory, whose results are comparable with those of chromatography, besides it requires low volumes of reagent and sample. Some of the procedures employed in this analysis are based on the reduction of nitrate to nitrite ions, for example by passing the samples through a cadmium-copper reduction column, with subsequent photometric determination of the formed nitrite using colour-forming reagents. One of the drawbacks of this method is that the sensitivity decreases for high nitrate concentrations. Spectrophotometry is often used for

* Corresponding author.
*E-mail address:* sgarcia@criba.edu.ar (S.G. García).

https://doi.org/10.1016/j.rineng.2022.100800
Received 11 September 2022; Received in revised form 19 November 2022; Accepted 25 November 2022
Available online 26 November 2022

nitrate/nitrite detection due to its simplicity, but many of the applied procedures are time consuming and vulnerable to interferences caused by different ions. They are based mainly on the reaction of the anion with detecting reagents, and the subsequent measurement of the absorbance of the formed product, which is proportional to anion concentration. Nevertheless, these methods are not suitable for in-situ measurements.

Recently, electromagnetic sensors and biosensors have been developed, which present the possibility of measuring in-situ. Electromagnetic sensors measure physical properties in terms of impedance, being highly reliable and low cost, with fast response. However, these sensors have some drawbacks such as the variation of the impedance that changes according to the sensor configuration and leading to sensitivity modifications, and the environmental conditions (temperature, presence of contaminants/ions), that affect the measurement precision. As for the biosensors, based on the interaction of nitrate ions with biological material, they show better results than electromagnetic sensors in terms of sensitivity. However, these biosensors are expensive and produce chemical waste.

The electrochemical techniques for detection of these anions have shown to have a good sensitivity and a simple operation in comparison with other methods, eliminating toxic reagents in the nitrate measurements or toxic wastes [14]. The electrochemical system has the ability to convert the nitrate anions into a potential difference, current or impedance. Furthermore, in the recent years the miniaturization capacity of electrochemical sensors has been demonstrated, reporting excellent results in the detection of nitrate ions [16,17].

The use of electrodeposited metal nanoparticles like electrocatalyst material for nitrate reduction, has been reported in numerous articles due to it allows the control of the morphological features of the material through the adjustment of parameters such as pH [18–20], potential [21,22], type of precipitant and additives [23], electrolyte composition [24], and electrolyte supports [25,26]. In turn, these structural properties have a huge role in the ability of the material as electrocatalyst [27].

Previous works have proved the high performance of supported copper nanostructures as an electrocatalyst material for reduction of nitrate ions, including different substrates such as metals [28–30], boron-doped diamond (BDD) [31], stainless steel [32], and different types of carbonaceous substrates like glassy carbon (GC) [33,34], graphite [35], highly oriented pyrolytic graphite (HOPG) [36], and graphene oxide (GO) [37,38]. In all cases, acceptable results of nitrate detection have been obtained, being relevant to carry out a comparison study between them.

The use of different anions for the electrodeposition of copper nanoparticles has been studied, comparing the effects of non-complex anions like $ClO_4^-$, $NO_3^-$ and $SO_4^{2-}$ [39–42]. Even though sulfate anions have shown to exhibit a greater adsorption on the substrate surface than the other anions, it has been widely used for copper electrodeposition on carbonaceous substrates, both as copper salt and as a part of supporting electrolyte [43–48].

The aim of the present work is to carry out a comparative analysis of the formation of CuNPs by electrodeposition, using different substrates (HOPG and VC), and supporting electrolytes containing the $SO_4^{2-}$ anions ($Na_2SO_4$ and $H_2SO_4$). The nucleation and growth process was studied by conventional electrochemical techniques (cyclic voltammetry and chronoamperometry), and the obtained nanostructures are characterized by scanning electron microscopy (SEM). The electrocatalytic effect of the systems towards the reduction of $NO_3^-$ anions, was evaluated qualitatively by cyclic voltammetry.

## 2. Experimental

The electrocrystallization of copper was carried out in a conventional three-electrode electrochemical cell at a temperature of $T = 298$ K. The working electrodes were HOPG and VC, both inserted into a Teflon holder, providing an exposed area of 0.1633 $cm^2$ and 0.0794 $cm^2$, respectively. The VC electrode surface was mechanically polished with emery paper of progressively finer grain size, followed by 0.3 μm alumina paste, and then rinsed with tri-distilled water. The HOPG electrode (SPI II grade, SPI Supplies, USA) was a sheet prepared by cleaving the first layers of the surface with a piece of sticky tape immediately prior to use. A Saturated Calomel Electrode (SCE) and a Pt sheet (1 $cm^2$), were used as reference and counter electrode, respectively. All electrode potentials mentioned in this work, are referred to SCE. The solutions used for copper electrodeposition were:

i) 1 mM $CuSO_4$ + 0.1 M $Na_2SO_4$
ii) 1 mM $CuSO_4$ + 0.1 M $H_2SO_4$ and for the electrocatalytic analysis:
iii) 0.1 M $NaNO_3$ + 0.1 M $Na_2SO_4$

All the electrolytic solutions were prepared with ultrapure chemicals (E. Merck, Darmstadt) and tri-distilled water. Prior to each experiment, the solutions were deaerated by nitrogen bubbling.

Cyclic voltammetric measurements and chronoamperometric studies were performed using a computer-controlled EG&G Princeton Applied Research model 273 A potentiostat-galvanostat. The morphology of supported copper nanoparticles was analyzed by scanning electron microscopy (SEM) with a Zeiss MA 10 microscope. The catalytic activity of the CuNPs-modified electrodes was evaluated qualitatively by cyclic voltammetry.

## 3. Results and discussion

### 3.1. Voltammetry

Cyclic voltammetry was used to analyze the electrodeposition of Cu on HOPG and VC substrates, from solutions with different supporting electrolytes. Fig. 1a) shows cyclic voltammograms of the system HOPG/Cu from 1 mM $CuSO_4$ + 0.1 M $Na_2SO_4$ solution (solution i). In the negative scan direction, a cathodic peak is observed, which corresponds to Cu reduction according to the reaction (1), and in the reverse scan, the oxidation of Cu is evidenced by an anodic peak at $E = 0.09$ V.

$$Cu^{2+} + 2e \rightarrow Cu \quad (1)$$

Voltammetric results with different features are also shown in Fig. 1a for the system VC/Cu. A small peak appears at a potential value of 0.1 V, followed by a more noticeable peak, which can be associated to the reduction of $Cu^{+2}$ to $Cu^+$ (reaction 2), and of $Cu^+$ to Cu (reaction 3), respectively. It is well known that in certain cases, the copper ions discharge taking place in two steps, is evident in cyclic voltammograms [39,49,50].

$$Cu^{2+} + 2e \rightarrow Cu^+ \quad (2)$$

$$Cu^+ + 2e \rightarrow Cu \quad (3)$$

The voltammetric response for HOPG and VC electrodes in the solution containing 1 mM $CuSO_4$ + 0.1 M $H_2SO_4$ (solution ii) is exhibited in Fig. 1b. A different behavior is observed in both cases, *i.e.*, the formation of Cu deposits on HOPG begins at potentials more negative than in the solution i, while for VC, the peaks representing the two reduction stages are observed separately. The process is favored in VC and it could be explained by considering the existence of structural defects in the VC surface, which would facilitate Cu nucleation [40]. It is well known that HOPG surfaces may have structural defects such as edge planes, ridges, fissures or cracks, which play an important role during the initial stages of metal nucleation and growth. This fact is attributed to the polar C–O functional groups (hydroxyl, carbonyl, carboxylate, etc.) terminating the defects sites, that influencing the metal adsorption. The difference with VC surfaces is related to the fact that, due to its manufacturing method, the VC is more disordered not only microstructurally but also

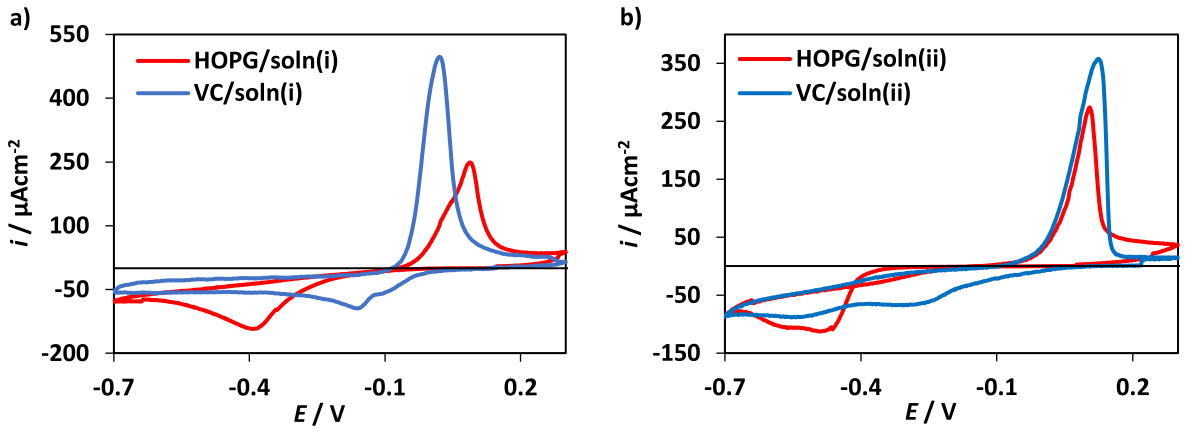


**Fig. 1.** Cyclic voltammograms for Cu electrodeposition in 1 mM $CuSO_4$ with a) 0.1 M $Na_2SO_4$ (soln. i) and b) 0.1 M $H_2SO_4$ (soln. ii), at $|dE/dt| = 10$ mV $s^{-1}$, on HOPG and VC electrodes.

electronically than HOPG, promoting the nucleation process [51–54]. Also, Bolzán [47] reported that probably, carbonyl groups are the most effective sites for the electron transfer and they may determine the number of nucleation sites for copper electrodeposition.

Anyway, for both carbonaceous substrates, it was found that the solution containing $Na_2SO_4$ as supporting electrolyte is more effective because the process occurs at more positive potential values. From these results, it could be inferred that, in the presence of $H_2SO_4$ as supporting electrolyte, the $SO_4^{2-}$ anions could be adsorbed on the surface, blocking active sites for copper deposition [36,41,42].

### 3.2. Chronoamperometric results

The metal electrodeposition usually occurs through nucleation and growth mechanisms and the current transients can provide useful information about the process. For this reason, typical current transients were peformed for Cu on HOPG and VC electrodes. All of them were characterized by a gradual current increase until a maximum is reached within the final portion falling according to the Cottrell equation [55]. Fig. 2a shows representative experimental transients for Cu on HOPG and VC electrodes in the solution i, at $E = -0.42$ V, selected in a region after the reduction peak in cyclic voltammograms. The current maximum for VC substrate is $i_m = -420.75$ µAcm$^{-2}$ at $t_m = 0.18$ s, while for HOPG, although a greater maximum current peak is obtained ($i_m = -702.39$ µAcm$^{-2}$), it is reached at longer times ($t_m = 0.22$s). This difference could be associated to the presence of the first stage of the deposition process (eqn. (2)), considered the rate-determining stage [39,49,50], in which the $Cu^+$ ions could be adsorbed on the VC surface until a more negative potential is reached and a total discharge of this intermediate specie is produced.

The transients for both electrodes carried out at a more negative potential value ($E = -0.55$ V) in the solution ii, are presented in Fig. 2b. In this case, the maximum current as well as the time when this maximum occurs, are similar. This behavior could be interpreted considering that, as the number of active sites depends on the electrode potential [43], Cu nuclei population increases as the deposition potential becomes more negative, leading to quite similar $i_m$ and $t_m$ values for VC and HOPG substrates.

In order to obtain some information about the kinetics of the electrodeposition process, the model proposed by Sharifker and Hills [56] was used to determine the type of nucleation and growth mechanism, instantaneous or progressive. For this study, experimental transients were compared with dimensionless curves plotted according to the following equations:

$$\frac{i^2}{i_m^2} = \frac{1.9542}{\frac{t}{t_m}}\left\{1 - \exp\left[-1.2564\left(\frac{t}{t_m}\right)\right]\right\}^2 \quad instantaneous \tag{1b}$$

$$\frac{i^2}{i_m^2} = \frac{1.2254}{\frac{t}{t_m}}\left\{1 - \exp\left[-2.3367\left(\frac{t}{t_m}\right)^2\right]\right\}^2 \quad progressive \tag{2b}$$

where $i_m$ and $t_m$ are the peak coordinates, namely the maximum current density and the time where this current is reached, respectively.

Fig. 3a shows the comparison of the experimental current transients

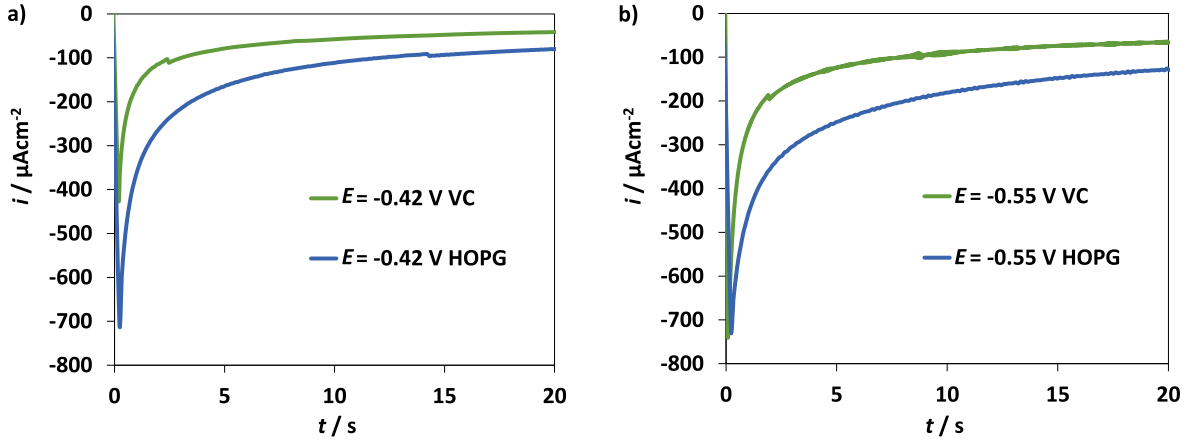


**Fig. 2.** Representative experimental current transients for Cu electrodeposition on HOPG and VC electrodes in a) 1 mM $CuSO_4$ with 0.1 M $Na_2SO_4$ (soln. i) and b) 0.1 M $H_2SO_4$ (soln. ii) solutions.

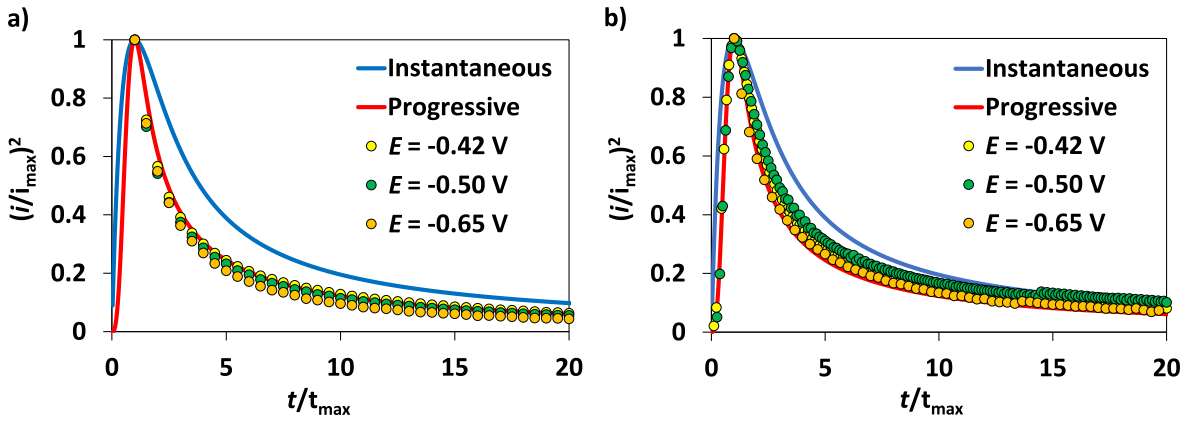


**Fig. 3.** Comparison of experimental transients with theoretical curves for Cu electrodeposition on HOPG in a) soln. i and b) soln. ii.

recorded during the electrodeposition of Cu on HOPG electrode from the solution i, at different potentials, with the theoretical dimensionless curves obtained from eqns. (1) and (2). It was evidenced that this process follows a progressive nucleation mechanism for the three potentials values. For the solution ii, the metal electrodeposition occurs through a model of progressive nucleation at $E = -0.65$ V. At more positive potentials, the nucleation follows initially a progressive type mechanism at short times, passing through a transition zone and reaching instantaneous nucleation at longer times (Fig. 3b).

For the CuNPs/VC modified electrode, obtained from solution i, the electrodeposition process follows a progressive nucleation mechanism for the applied potentials values (Fig. 4a), as for the system CuNPs/HOPG. An intermediate mechanism between progressive and instantaneous was obtained when the solution ii was used for the generation of copper deposits (Fig. 4b).

### 3.3. Surface analysis

A morphological analysis of the surface electrode after applying a simple potentiostatic pulse in the studied electrolytic solutions, was carried out by SEM, in order to analyze the effect of the substrate in the process and to validate the nucleation mechanism type.

The copper crystals obtained on HOPG from both solutions containing $Na_2SO_4$ and $H_2SO_4$ (pulse parameters: $E = -0.65$ V, $t = 400$ s), together with the corresponding histograms, are exhibited in Fig. 5. Regarding the crystal size, the presence of particle with different diameters corroborates clearly the progressive type mechanism derived by the Sharifker and Hills model, i.e. new nuclei are continuously generated during the whole deposition process.

A great density of hemispherical particles distributed on the substrate is observed for the Cu deposits generated from solutions containing $Na_2SO_4$ (Fig. 5a), while for those formed from the acid solution, the existence of small nanocrystals coexisting with larger particles is evidenced, which grow forming aligned agglomerates, preferably on edges steps of the HOPG substrate (Fig. 5b). The presence of particles with different sizes indicates that a progressive type mechanism prevails, corroborating clearly the one derived by the Sharifker and Hills model. The covered area for both systems was estimated, resulting in 16.4% and 20.8% of the geometric area, respectively. From the corresponding histograms, a larger number of small particles with diameters 33–50 nm were evidenced for the copper deposits.

Fig. 6a shows a representative SEM micrograph of Cu-decorated VC electrode, obtained after applying a potentiostatic pulse of $E = -0.42$ V, with a deposition time of $t = 450$ s, to the substrate. The crystals exhibit a dendritic morphology consisting in a flower-like shape, randomly distributed on the substrate surface. This type of deposits was also observed by Grujicic and Pesic [43] on VC, and it can be attributed to initially formed Cu nuclei by disproportionation of $Cu^{+}$, which coexist with smaller crystallites resulting of direct reduction of $Cu^{2+}$. This assumption is also supported by the voltammetric and chronoamperometric results obtained for this system. The particle size distribution reveals a large number of small particles with diameters 38–50 nm and some large ones with diameters up to 299 nm. In this case, the calculated covered area was 8.1% of the geometric area. When the deposits were formed at $E = -0.65$ V, $t = 450$ s, a larger number of small particles of about 31 nm and a larger particle density are evidenced, with a covered area of 15%. In this case, the number of particles with a diameter greater than 130 nm is negligible.

From SEM analysis, it can be observed that in the sulfate solution as well as in the acid electrolyte, the Cu electrodeposition process on HOPG substrates does not present significant changes regarding the morphological features, finding, in both cases, hemispherical nanoparticles

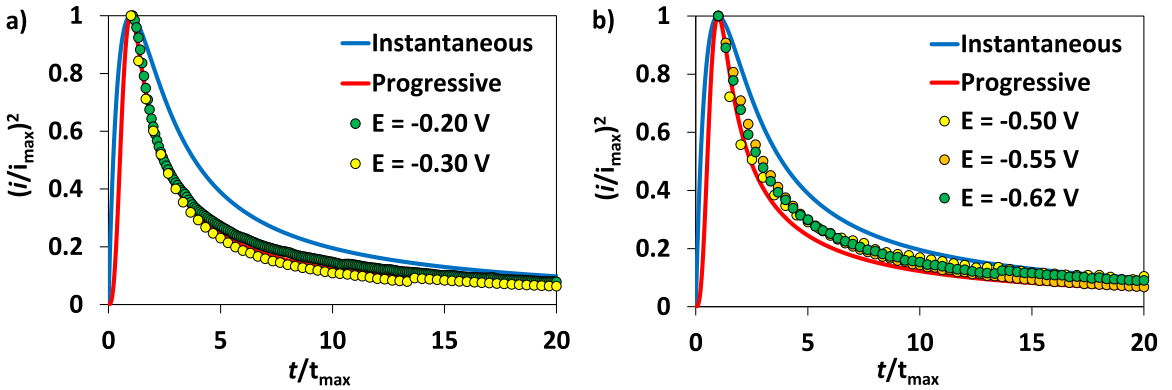


**Fig. 4.** Comparison of experimental transients for Cu electrodeposition on the VC substrate with theoretical curves in: a) soln. i and b) soln. ii.

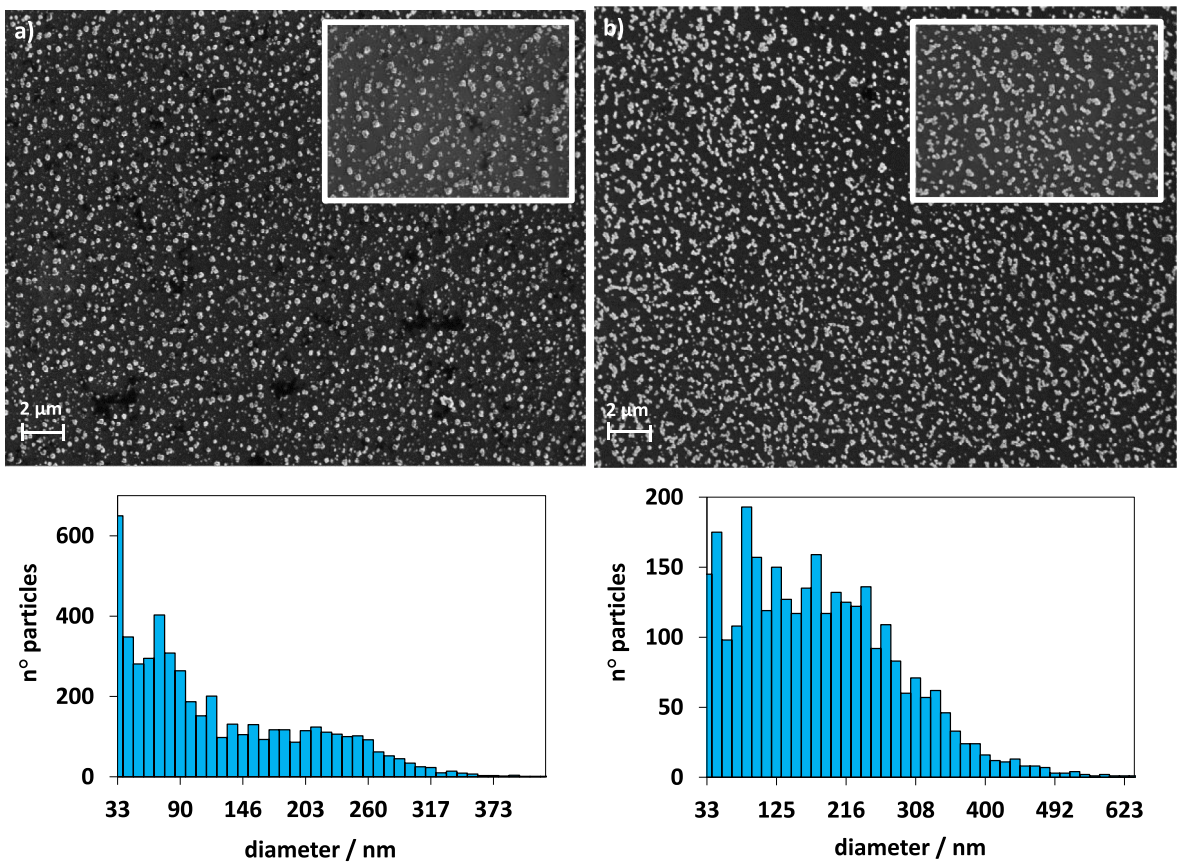


**Fig. 5.** SEM images of Cu deposits on HOPG electrode obtained from solutions: a) 1 mM $CuSO_4$ + 0.1 M $Na_2SO_4$ and b) 1 mM $CuSO_4$ + 0.1 M $H_2SO_4$, with the corresponding histograms. Inside: 30Kx magnification.

distributed preferentially on the step edges of the surface. However, relevant differences in the Cu nucleation and growth process on VC surfaces, are evidenced both in the distribution and in the size of the nuclei formed. Cu crystallites are randomly distributed on the surface due to the different location of the active nucleation centers on its surface. For the system generated from the $Na_2SO_4$ electrolytic solution, flower-shaped dendritic structures were found , while for acid solutions, a large amount of small CuNPs distributed on the surface was detected. The marked influence of the electrolytic solutions on the deposits morphology on VC can be related to the defects of substrate, which could interact with the electrolytic media directing the nucleation and growth of the crystallites in different ways [23].

### 3.4. Electrocatalysis

The electrocatalytic effect of the supported CuNPs formed from the different supporting electrolytes on HOPG and VC electrodes, was verified qualitatively by cyclic voltammetry. Fig. 7 shows voltammetric results for CuNPs in 0.1 M $NaNO_3$ + 0.1 M $Na_2SO_4$ and 0.1 M $Na_2SO_4$ solutions. In the blank electrolyte (inset), featureless voltammograms were observed in the potential region $-0.2 \leq E/V \leq -1$. At more negative potential values, a cathodic current increase is evidenced, related to the hydrogen evolution reaction. In the presence of nitrate ions a cathodic peak was registered related to the reduction nitrate reaction. An enhancement in the catalytic activity for the reduction of $NO_3^-$ anions was evidenced when the particles were generated on HOPG from solution i (Fig. 7a). For solution ii (Fig. 7b), the voltammetric response for the CuNPs/VC modified electrode evidenced a behavior similar to that of the CuNPs/HOPG system, although in the latter, the anion reduction reaction starts earlier ($E = -0.51$ V).

Therefore, it could be considered that the use of HOPG as a support for CuNPs prepared from either electrolytes, results in a good electrocatalyst material for nitrate reduction reaction. Unlike HOPG, it could be possible to use VC as support for only the CuNPs generated from the solution containing sulfuric acid. From these results, it could be inferred that the presence of predominantly small particles, and consequently a larger covered area, enhanced the catalytic activity for the nitrate reaction.

## 4. Conclusions

Copper electrodeposition occurs in a single stage for HOPG in the studied solutions, while for the VC substrate the presence of two stages of the reduction process, were evidenced. In both substrates, it was found that the solution containing $Na_2SO_4$ is more effective because copper reduction occurs at more positive potential values, being the most favored process in VC due to the existence of defects in its structure, which would facilitate Cu nucleation.

The kinetics of nucleation and growth of CuNPs on HOPG was predominantly progressive, presenting a good correlation with SEM images of the crystals. HOPG showed a preferential distribution of hemispherical nanoparticles on the step edges of the electrode surface for both electrolyte solutions used. In the case of VC, the nucleation mechanism varied from progressive to instantaneous mode, not leading to conclusive results. The deposits presented different morphology distribution in both substrates, showing flower-shaped dendritic structures for the deposits generated from $Na_2SO_4$ solutions and randomly distributed hemispherical particles for the acid electrolytes with a large number of small NPs.

The modified HOPG/CuNPs and CV/CuNPs electrodes showed a catalytic effect for the reduction of nitrate, evidencing an enhancement in the catalytic activity when the particles were generated on HOPG

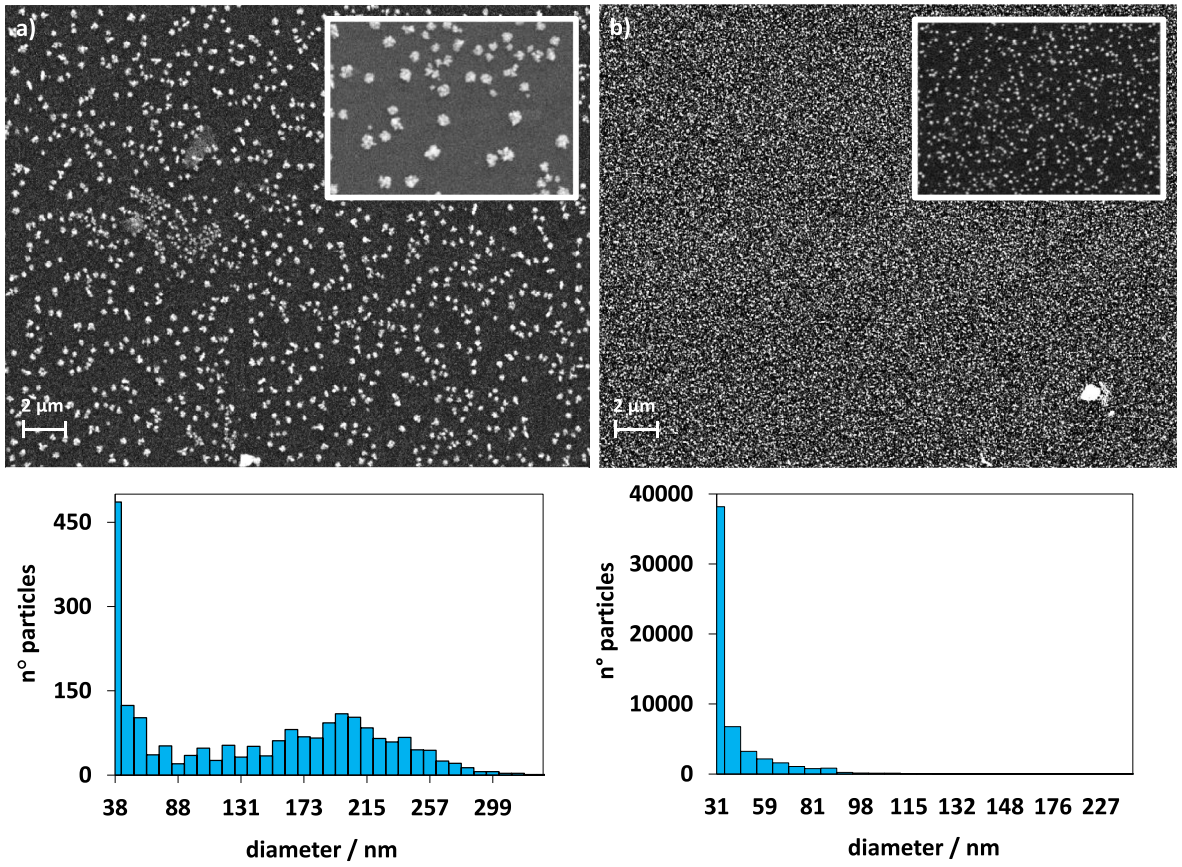


**Fig. 6.** SEM images of Cu deposits on VC electrode obtained from solutions: a) 1 mM $CuSO_4$ + 0.1 M $Na_2SO_4$ and b) 1 mM $CuSO_4$ + 0.1 M $H_2SO_4$, with the corresponding histograms. Inside: 50Kx magnification.

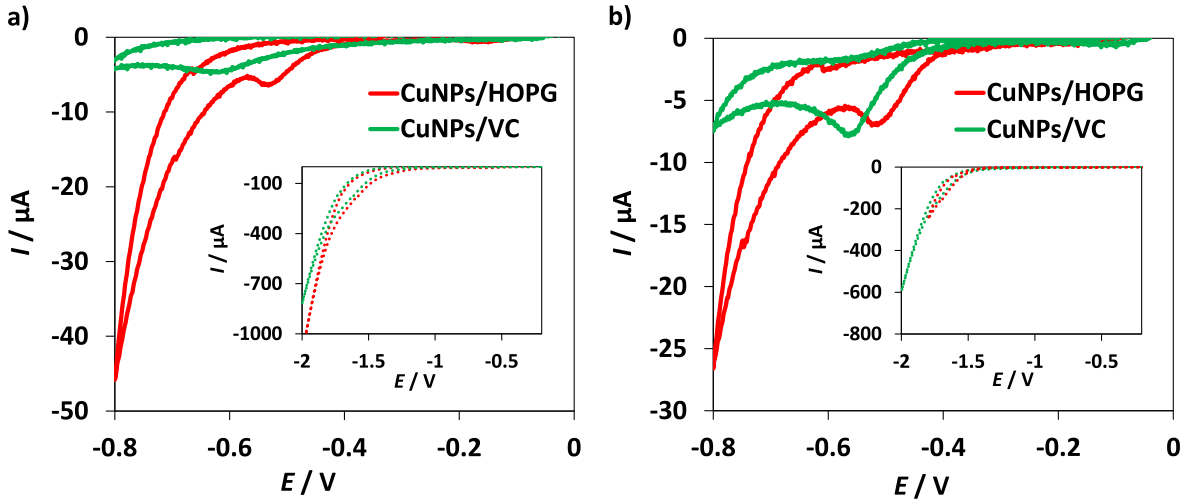


**Fig. 7.** Cyclic voltammograms for CuNPs in 0.1 M $NaNO_3$ + 0.1 M $Na_2SO_4$ solution, prepared with (a) soln. i and (b) soln. ii, on HOPG and VC electrodes.|d$E$/dt| = 20 mV $s^{-1}$. Inset: The same systems in blank electrolytes.

from solutions containing $Na_2SO_4$. In the presence of $H_2SO_4$ as supporting electrolyte, similar maximum reduction currents were obtained for HOPG and VC modified substrates.

## Credit author statement

N. Zurita: Investigation, Writing - Original Draft. The subject of this work is part of her doctoral thesis; S. García: Supervision, Writing - Review & Editing, Project administration.

## Declaration of competing interest

The authors declare that they have no known competing financial interests or personal relationships that could have appeared to influence the work reported in this paper.

## Data availability

No data was used for the research described in the article.

## Acknowledgments

The authors wish to thank the Universidad Nacional del Sur (Argentina) for the financial support of this work. N. Zurita acknowledges a fellowship granted by CIC (Comisión de Investigacionaes Científicas de la Provincia de Buenos Aires).

## References

[1] J. Mateo-Sagasta, S.M. Zadeh, H. Turral, J. Burke, Water Pollution from Agriculture: A Global Review, Food and Agriculture Organization of the United Nations, 2017. https://www.fao.org/3/i7754e/i7754e.pdf.
[2] T. Addiscott, A.j. Gold, C. Oviatt, N. Benjamin, K. Giller, Nitrate, Agriculture and the Environment, CABI Publishing, 2005. http://sherekashmir.informaticspublishing.com/597/1/9780851999135.pdf.
[3] K. Parris, Impact of agriculture on water pollution in OECD countries: recent trends and future prospects, Int. J. Water Resour. Dev. 27 (1) (2011) 33–52, https://doi.org/10.1080/07900627.2010.531898.
[4] J. Mateo-Sagasta, S.M. Zadeh, H. Turral, More People, More Food, Worse Water? A Global Review of Water Pollution from Agriculture, Food and Agriculture Organization of the United Nations, 2018. https://www.iwmi.cgiar.org/Publications/Books/PDF/more-people-more-food-worse-water.pdf.
[5] M. Parvizishad, A. Dalvand, A.H. Mahvi, F. Goodarzi, A Review of Adverse Effects and Benefits of Nitrate and Nitrite in Drinking Water and Food on Human Health, Health Scope, 2017, https://doi.org/10.5812/jhealthscope.14164.
[6] M.H. Ward, R.R. Jones, J.D. Brender, et al., Drinking water nitrate and human health: an updated review, Int. J. Environ. Res. Publ. Health 15 (7) (2018), https://doi.org/10.3390/ijerph15071557.
[7] P. Li, X. He, W. Guo, Spatial groundwater quality and potential health risks due to nitrate ingestion through drinking water: a case study in Yan'an City on the Loess Plateau of northwest China, Hum. Ecol. Risk Assess. 25 (1–2) (2019) 11–31, https://doi.org/10.1080/10807039.2018.1553612.
[8] M. Qasemi, M. Farhang, H. Biglari, et al., Health risk assessments due to nitrate levels in drinking water in villages of Azadshahr, northeastern Iran, Environ. Earth Sci. 77 (23) (2018) 1–9, https://doi.org/10.1007/s12665-018-7973-6.
[9] World Health Organization, Guidelines for Drinking-Water Quality, World Health Organization, 2011. https://apps.who.int/iris/bitstream/handle/10665/44584/9789241548151_eng.pdf.
[10] C. Lowe, J. Kurscheid, A. Lal, et al., Health risk assessment for exposure to nitrate in drinking water in Central Java, Indonesia, Int. J. Environ. Res. Publ. Health 18 (5) (2021) 1–10, https://doi.org/10.3390/ijerph18052368.
[11] A. Temkin, S. Evans, T. Manidis, C. Campbell, O v Naidenko, Exposure-based assessment and economic valuation of adverse birth outcomes and cancer risk due to nitrate in United States drinking water, Environ. Res. 176 (2019), 108442, https://doi.org/10.1016/j.envres.2019.04.009.
[12] J. Schullehner, B. Hansen, M. Thygesen, C.B. Pedersen, T. Sigsgaard, Nitrate in drinking water and colorectal cancer risk: a nationwide population-based cohort study, Int. J. Cancer 143 (1) (2018) 73–79, https://doi.org/10.1002/ijc.31306.
[13] Q.H. Wang, L.J. Yu, Y. Liu, et al., Methods for the detection and determination of nitrite and nitrate: a review, Talanta 165 (2017) 709–720, https://doi.org/10.1016/j.talanta.2016.12.044.
[14] M.E.E. Alahi, S.C. Mukhopadhyay, Detection methods of nitrate in water: a review, Sens. Actuator A Phys. 280 (2018) 210–221, https://doi.org/10.1016/j.sna.2018.07.026.
[15] C. Jiang, Y. He, Y. Liu, Recent advances in sensors for electrochemical analysis of nitrate in food and environmental matrices, Analyst 145 (16) (2020) 5400–5413, https://doi.org/10.1039/D0AN00823K.
[16] Y. Li, J. Sun, Y. Song, C. Bian, H. Dong, S. Xia, Determination of nitrate in potable water using a miniaturized electrochemical sensor, in: 2018 IEEE 13th Annual International Conference on Nano/Micro Engineered and Molecular Systems (NEMS), 2018, pp. 619–622, https://doi.org/10.1109/NEMS.2018.8557007.
[17] Z. Ren, Y. Li, A miniaturized electrochemical nitrate sensor and the design for its automatic operation based on distributed model, Math. Probl Eng. 2022 (2022) 1–9, https://doi.org/10.1155/2022/6028110.
[18] J.A.M. Oliveira, A.F. de Almeida, A.R.N. Campos, S. Prasad, J.J.N. Alves, R.A.C. de Santana, Effect of current density, temperature and bath pH on properties of Ni–W–Co alloys obtained by electrodeposition, J. Alloys Compd. 853 (2021), 157104, https://doi.org/10.1016/j.jallcom.2020.157104.
[19] Y.E. Sknar, I.v. Sknar, O.O. Savchuk, F.I. Danilov, Electrodeposition of Ni-Co alloy from methansulfonate electrolyte. The role of the electrolyte pH in the anomalous codeposition of nickel and cobalt, Surf. Coat. Technol. 387 (2020), 125542, https://doi.org/10.1016/j.surfcoat.2020.125542.
[20] S.M. Jesmani, H. Mohammadian-Semnani, H. Abdollah-Pour, R. Amini, The effect of pH on electrocatalytic properties of electrodeposited Ni-Mo/Ni coating using 1-ethyl-3-methylimidazolium bromide, Mater. Res. Express 6 (10) (2019) 1065e2, https://doi.org/10.1088/2053-1591/ab2139.
[21] X. Zhang, K. Wan, P. Subramanian, M. Xu, J. Luo, J. Fransaer, Electrochemical deposition of metal-organic framework films and their applications, J. Mater. Chem. 8 (16) (2020) 7569–7587, https://doi.org/10.1039/d0ta00406e.
[22] M.B. Kale, R.A. Borse, A. Gomaa Abdelkader Mohamed, Y. Wang, Electrocatalysts by electrodeposition: recent advances, synthesis methods, and applications in energy conversion, Adv. Funct. Mater. 31 (25) (2021), https://doi.org/10.1002/adfm.202101313.
[23] N. Girija, S.S. Kuttan, B.N. Nair, U.N. Saraswathy Hareesh, Morphology control in nickel cobaltite synthesized via solution routes for electrochemical applications, Results in Eng 15 (2022), 100536, https://doi.org/10.1016/j.rineng.2022.100536.
[24] N.M. Shokobayev, A.E. Nurtazina, O.S. Kholkin, A.Z. Abilmagzhanov, N.S. Ivanov, I.E. Adelbaev, Obtaining of copper powder by method of a vortex electrolysis from acid sulphate electrolytes, Results in Eng 16 (2022), 100604, https://doi.org/10.1016/j.rineng.2022.100604.
[25] N.D. Zakaria, M.H. Omar, N.N. Ahmad Kamal, et al., Effect of supporting background electrolytes on the nanostructure morphologies and electrochemical behaviors of electrodeposited gold nanoparticles on glassy carbon electrode surfaces, ACS Omega 6 (38) (2021) 24419–24431, https://doi.org/10.1021/acsomega.1c02670.
[26] S. Demoustier-Champagne, P.Y. Stavaux, Effect of electrolyte concentration and nature on the morphology and the electrical properties of electropolymerized polypyrrole nanotubules, Chem. Mater. 11 (3) (1999) 829–834, https://doi.org/10.1021/cm9807541.
[27] Z. Cai, Y. Ye, X. Wan, et al., Morphology–dependent electrochemical sensing properties of iron oxide–graphene oxide nanohybrids for dopamine and uric acid, J. Nanomater. 9 (6) (2019) 835, https://doi.org/10.3390/nano9060835.
[28] M.A. Hasnat, S. ben Aoun, S.M. Nizam Uddin, et al., Copper-immobilized platinum electrocatalyst for the effective reduction of nitrate in a low conductive medium: mechanism, adsorption thermodynamics and stability, Appl. Catal. Gen. 478 (2014) 259–266, https://doi.org/10.1016/j.apcata.2014.04.017.
[29] Y. Li, J.Z. Sun, C. Bian, et al., Copper nano-clusters prepared by one-step electrodeposition and its application on nitrate sensing, AIP Adv. 5 (4) (2015), 041312, https://doi.org/10.1063/1.4905712.
[30] M. Hou, Y. Pu, Qi W. kang, et al., Enhanced electrocatalytic reduction of aqueous nitrate by modified copper catalyst through electrochemical deposition and annealing treatment, Chem. Eng. Commun. 205 (5) (2018) 706–715, https://doi.org/10.1080/00986445.2017.1413357.
[31] R.G. Compton, C.M. Welch, M.E. Hyde, C.E. Banks, The detection of nitrate using in-situ copper nanoparticle deposition at a boron doped diamond electrode, Anal. Sci. 21 (2005) 1421–1430, https://doi.org/10.2116/analsci.21.1421.
[32] Y.J. Shih, Z.L. Wu, C.Y. Lin, Y.H. Huang, C.P. Huang, Manipulating the crystalline morphology and facet orientation of copper and copper-palladium nanocatalysts supported on stainless steel mesh with the aid of cationic surfactant to improve the electrochemical reduction of nitrate and N2 selectivity, Appl. Catal., B 273 (2020), 119053, https://doi.org/10.1016/j.apcatb.2020.119053.
[33] A.O. Solak, P. Çekirdek, Square wave voltammetric determination of nitrate at a freshly copper plated glassy carbon electrode, Anal. Lett. 38 (2) (2005) 271–280, https://doi.org/10.1081/AL-200045149.
[34] A.O. Solak, Gülser Pi, E. Gökm, F. Gökmesşe, A new differential pulse voltammetric method for the determination of nitrate at a copper plated glassy carbon electrode, Mikrochim. Acta 134 (1–2) (2000) 77–82, https://doi.org/10.1007/s006040070057.
[35] M.R. Majidi, K. Asadpour-Zeynali, B. Hafezi, Fabrication of nanostructured copper thin films at disposable pencil graphite electrode and its application to elecrocatalytic reduction of nitrate, Int. J. Electrochem. Sci. 6 (1) (2011) 162–170. http://www.electrochemsci.org/papers/vol6/6010162.pdf.
[36] N. Zurita, S.G. García, Influence of supporting electrolyte on electrochemical formati-on of copper nanoparticles and their electrocatalytic properties, J. Electrochem. Sci. Eng. 12 (2) (2022) 253–264, https://doi.org/10.5599/jese.1077.
[37] C. Sun, F. Li, H. An, Z. Li, A.M. Bond, J. Zhang, Facile electrochemical co-deposition of metal (Cu, Pd, Pt, Rh) nanoparticles on reduced graphene oxide for electrocatalytic reduction of nitrate/nitrite, Electrochim. Acta 269 (2018) 733–741, https://doi.org/10.1016/j.electacta.2018.03.005.
[38] J. Wang, Z. Zhang, S. Ding, Cu supported on the graphene oxide modified graphite felt electrode for highly efficient nitrate electroreduction, J. Environ. Chem. Eng. 10 (3) (2022), https://doi.org/10.1016/j.jece.2022.108092.
[39] L.H. Mendoza Huizar, C.H. Rios Reyes, D.E. Garcia Rodriguez, Tuning the copper cluster's size on Hopg by electrodeposition from perchlorate aqueous solutions. An AFM study, J. Serb. Chem. Soc. 84 (2019) 1–13, https://doi.org/10.2298/JSC190123054G.
[40] D.E. García-Rodríguez, L.H. Mendoza-Huizar, C.H. Rios-Reyes, M.A. Alatorre-Ordaz, Copper electrodeposition on glassy carbon and highly oriented pyrolytic graphite substrates from perchlorate solutions, Quim. Nova 35 (4) (2012) 699–704, https://doi.org/10.1590/S0100-40422012000400008.
[41] O. Ghodbane, L. Roué, D. Bélanger, Copper electrodeposition on pyrolytic graphite electrodes: effect of the copper salt on the electrodeposition process, Electrochim. Acta 52 (19) (2007) 5843–5855, https://doi.org/10.1016/j.electacta.2007.03.009.
[42] J. Vazquez-Arenas, G. Vázquez, A.M. Meléndez, I. González, The effect of the Cu2+/Cu+ step on copper electrocrystallization in acid noncomplexing electrolytes, J. Electrochem. Soc. 154 (9) (2007) D473, https://doi.org/10.1149/1.2755873.
[43] D. Grujicic, B. Pesic, Electrodeposition of copper: the nucleation mechanisms, Electrochim. Acta 47 (18) (2002) 2901–2912, https://doi.org/10.1016/S0013-4686(02)00161-5.
[44] N. Bommireddy, S.K. Palathedath, Templated bimetallic copper-silver nanostructures on pencil graphite for amperometric detection of nitrate for aquatic monitoring, J. Electroanal. Chem. (2020) 856, https://doi.org/10.1016/j.jelechem.2019.113660.
[45] D. Yin, Y. Liu, P. Song, et al., In situ growth of copper/reduced graphene oxide on graphite surfaces for the electrocatalytic reduction of nitrate, Electrochim. Acta 324 (2019), https://doi.org/10.1016/j.electacta.2019.134846.
[46] R.C. Tangirala, C.T.J. Low, C. Ponce-De-León, S.A. Campbell, F.C. Walsh, Copper deposition at segmented, reticulated vitreous carbon cathode in Hull cell, Trans.

Inst. Met. Finish. 88 (2) (2010) 84–92, https://doi.org/10.1179/174591910X12646070884872.
[47] A.E. Bolzán, Electrodeposition of copper on glassy carbon electrodes in the presence of picolinic acid, Electrochim. Acta 113 (2013) 706–718, https://doi.org/10.1016/j.electacta.2013.09.132.
[48] L. Huang, E.S. Lee, K.B. Kim, Electrodeposition of monodisperse copper nanoparticles on highly oriented pyrolytic graphite electrode with modulation potential method, Colloids Surf. A Physicochem. Eng. Asp. 262 (1–3) (2005) 125–131, https://doi.org/10.1016/j.colsurfa.2005.03.023.
[49] A. Milchev, T. Zapryanova, Nucleation and growth of copper under combined charge transfer and diffusion limitations: Part i, Electrochim. Acta 51 (14) (2006) 2926–2933, https://doi.org/10.1016/j.electacta.2005.08.045.
[50] R. Ghosh, V. Sudha, S. Harinipriya, Thermodynamic analysis of electrodeposition of copper from copper sulphate, Bull. Mater. Sci. 42 (2) (2019) 1–8, https://doi.org/10.1007/s12034-018-1712-1.
[51] R.L. McCreery, Advanced carbon electrode materials for molecular electrochemistry, Chem. Rev. 108 (7) (2008) 2646–2687, https://doi.org/10.1021/cr068076m.
[52] S. Ŝtrbac, Z. Rakočević, K.I. Popov, M.G. Pavlović, R. Petrović, The role of surface defects in Hopg on the electrochemical and physical deposition of Ag, J. Serb. Chem. Soc. 64 (8) (1999) 483–493, https://doi.org/10.2298/JSC9908483S.
[53] D.Q. Yang, E. Sacher, Ar þ-induced surface defects on Hopg and their effect on the nucleation, coalescence and growth of evaporated copper, Surf. Sci. 516 (2002) 43–55, https://doi.org/10.1016/S0039-6028(02)02065-4.
[54] J. Xu, Q. Chen, G.M. Swain, Anthraquinonedisulfonate electrochemistry: a comparison of glassy carbon, hydrogenated glassy carbon, highly oriented pyrolytic graphite, and diamond electrodes, Anal. Chem. 70 (15) (1998) 3146–3154, https://doi.org/10.1021/ac9800661.
[55] A. Yamada, Y. Kato, T. Yoshikuni, Y. Tanaka, N. Tanaka, Computer-assisted measurement of ion-diffusion coefficients by use of the cottrell equation, Anal. Chim. Acta 112 (1) (1979) 55–63, https://doi.org/10.1016/S0003-2670(01)93029-6.
[56] B. Scharifker, G. Hills, Theoretical and experimental studies of multiple nucleation, Electrochim. Acta 28 (2) (1982) 879–889, https://doi.org/10.1016/-0013-4686(83)85163-9.